High temperature superconducting ball formation in low frequency ac fields

R. Tao, X. Xu, and E. Amr
Department of Physics, Temple University, Philadelphia, Pennsylvania 19122-6082, USA
(Received 5 February 2003; revised manuscript received 8 August 2003; published 3 October 2003)

The electric-field induced ball formation has been observed for high temperature superconducting (HTSC) powders in an ac field of low frequency. Different from a static electric field, the HTSC particles in the ac field first form chains along the field direction if the electric field is below a critical value, E_{c1}. As soon as the electric field exceeds E_{c1}, the chains are broken and the HTSC particles form balls. The ball size reduces with further increase of the electric field. E_{c1}, as a function of frequency, first drops from the value for the static electric field and then increases with the frequency. The ball-formation phenomenon comes from the interaction between Cooper pairs and the applied electric field. A positive surface energy associated with the induced surface charge distributions on superconductors is a possible explanation.

DOI: 10.1103/PhysRevB.68.144505 PACS number(s): 74.90.+n, 74.72.−h, 74.25.−q, 68.35.Md

I. INTRODUCTION

The recent discovery of formation of high temperature superconducting (HTSC) granular balls in a strong static electric field has received much attention.[1–4] This phenomenon is now found to be general for all superconductors, including low temperature superconductors such as Pb, type I superconductors, and V_3Ga, Nb-N, and Nb_3Sn, type II superconductors.[5]

The discovery is related to an important topic, the interaction between superconductors and a static or quasistatic electric field. The London brothers first suggested that superconductors and normal conductors could respond to static electric fields differently and a static electric-field could penetrate into superconductors as far as the magnetic penetration depth, much deeper than it penetrates into normal conductors. However, they later gave up the idea after their experiment failed to confirm the prediction.[6] Later work by Landau[7] and Pippard *et al.*[8] used a real current at a normal metal-superconductor interface to show the electric-field penetration effect indirectly.[9] Since the discovery of high temperature superconductors,[10,11] there have been extensive studies of the electric field effect in the high-T_c cuprates[12] and measurement of electric-field penetration into the superconducting surface of YBaCuO.[13] While some of these works remain controversial, they at least show the importance and breadth of the topic.

The electric-field induced formation of superconducting balls confirms that superconductors respond differently to an electric field than normal conductors. A static electric field induces surface charge distributions on both normal conductors and superconductors. However, when the applied static electric field is strong enough, the surface charge on superconducting particles produces a positive surface energy, which leads to the formation of granular balls and flat layers clinging to the electrodes. This positive surface energy is unique to superconductors. Normal metals in a static electric field do not have such a surface energy.

Moreover, the experiment has found that when the temperature rises above the superconducting transition temperature T_c, the ball-formation phenomenon disappears.[1,5] This further confirms that the electric-field induced formation of superconducting balls is a result of the interaction between a strong electric-field and Cooper pairs.

In this paper, we report our experiments on high temperature superconducting ball formation in an ac field of low frequency, up to 800 Hz. While the balls in the static field bounce between the two electrodes rapidly, they usually just oscillate locally in the ac field. This provides us an opportunity to study the relationship between the ball size, electric-field, and frequency. We have found that the ball formation in ac field of low frequency has many similarities to that in the static electric-field. There is also a critical electric-field E_{c1}, which is a function of frequency. The ball formation only occurs if the applied ac field is stronger than E_{c1}. On the other hand, there are some distinct or additional features for the ball formation in ac field. For example, in the ac field, the HTSC particles first form chains or columns along the field direction when the electric-field is below E_{c1}. This phenomenon is absent in the static field. As soon as the electric-field exceeds E_{c1}, the chains are broken and the HTSC particles then form balls.

The details of the experiments, including experimental setup, critical electric-field for the ball formation, and the effect of particle surface on the ball formation, are in Sec. II. In Sec. III, we will present our preliminary theoretical explanation for the experiments. Finally we will summarize both experiment and theoretical results in Sec. IV.

II. EXPERIMENT

A. Experimental setup

The particles used in our experiment, NBCO ($NdBa_2Cu_3O_x$, 99.9% purity), BSCCO ($Bi_2Sr_2CaCu_2O_{8+x}$, 99.9% purity), and YBCO ($YBa_2Cu_3O_{7-x}$, 99.99% purity), were provided by Superconductive Components, Inc (SCI), Columbus, OH. The scanning electron micrograph of BSCCO, NBCO, and YBCO are shown in Figs. 1(a), 1(b) and 1(c), respectively. The typical particle size is a couple of micrometers. The BSCCO particles are usually of flake shape, while the NBCO and YBCO particles are of irregular shape. These particles were prepared either by a solid-state

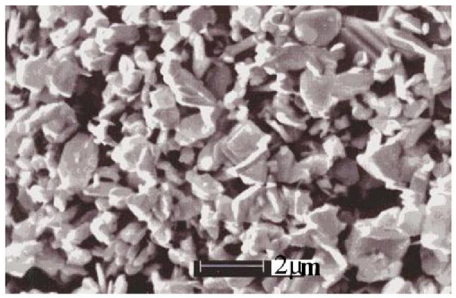

(a)

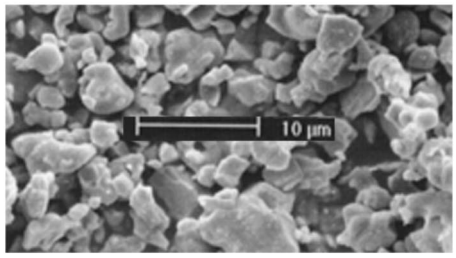

(b)

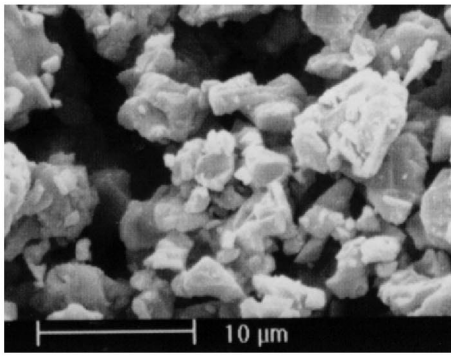

(c)

FIG. 1. (a) Scanning electronic micrograph of $Bi_2Sr_2CaCu_2O_{8+x}$, particles. (b) Scanning electronic micrograph of $NdBa_2Cu_3O_x$ particles. (c) Scanning electronic micrograph of $YBa_2Cu_3O_{7-x}$ particles.

method[14] or the Sandia Chemical Preparation.[15] NBCO, YBCO, and BSCCO have T_c around 94 K, 92 K, and 84 K, respectively.

Our experimental setup is sketched in Fig. 2. On a horizontal microscope teflon slide we mounted two parallel brass electrodes, which were 1 mm thick and about 4 mm apart.

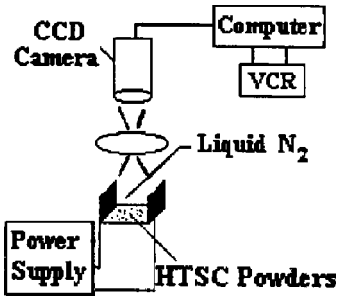

FIG. 2. The experimental setup.

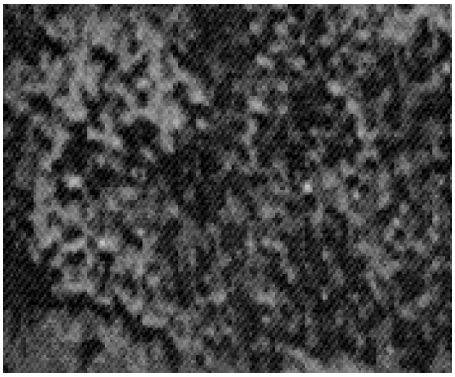

FIG. 3. The HTSC particles were well dispersed before the electric field was applied.

Three teflon spacers were used between the electrodes, one at the bottom and two at the two sides, to form a cell in a region of the most uniform electric-field. Only a small amount of a slurry of liquid nitrogen and HTSC particles was needed to fill the cell, measuring 4×5 mm^2 horizontally and 5 mm in vertical depth. The whole cell was submerged in liquid nitrogen. The top surface of the cell was open to allow liquid nitrogen to flow in so that a constant temperature was maintained at 77 K. The experiment was recorded by a high-speed video camera, which could take up to 1000 frames per second and enabled us to examine the dynamic process in detail.

As shown in Fig. 3, the HTSC particles were dispersed in liquid nitrogen before the ac electric-field was applied. In fact, the bubbles and constant movement of liquid nitrogen helped the dispersion of HTSC particles. In the experiment, for each selected frequency, we gradually increased the applied voltage and monitored the dynamic process through the high-speed camera. The frequency applied in our experiment was up to 800–1000 Hz, much smaller than ω_g, the superconducting energy-gap frequency.

B. Critical ac electric-field for the ball formation

As reported previously,[1,5] in the static field, there are two critical electric-fields, E_{c1} and E_{c2} with $E_{c1}<E_{c2}$. When the static field E is below E_{c1}, the superconducting powders do not aggregate into balls. The ball formation and the formation of layers clinging to the electrodes occur if $E\geqslant E_{c1}$. As the static field E increases, the balls get smaller, but are stable for $E_{c1}<E<E_{c2}$. If the static field E exceeds E_{c2}, the balls break into pieces and all the pieces fly to the electrodes and cling there.

The behavior of HTSC powder in an ac field of low frequency bears many similarities to the situation of static field. As the ac electric-field was gradually increasing, we noticed four different stages for the HTSC particles inside the electric-field.

(1) At very low applied electric-field, the HTSC particles did not move. It appeared that at this stage, the static friction between the HTSC particles and the bottom plate prevented the particles from moving.

(2) When the electric-field reached a particular value, the particles suddenly and quickly moved and formed chains or

FIG. 4. HTSC particles form chains and columns when the ac electric field is below the critical field for the ball formation. The bright spot was a bubble.

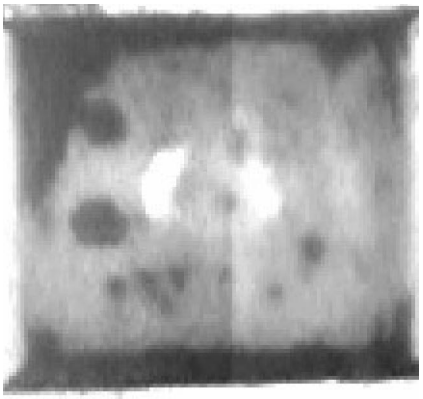

FIG. 5. As the ac field reaches the critical value, the HTSC particles form balls.

columns spanning between the two electrodes (Fig. 4). These structures were similar to the structure of electrorheological fluids formed in an electric-field.[16] This implies that the superconducting particles in the ac field are also polarized. The induced dipolar interactions lead to the chain structures. Such chain-column structures are absent in a static electric-field. There may be two reasons for this difference.

(a) In the static field, HTSC particles bounce between the two electrodes very fast; therefore, there is no chance for them to form chains and columns. For example, when a particle touches a positive electrode in a static field, it picks up a positive charge and, then, moves toward the negative electrode. Once the particle discharges and picks up a negative charge, it flies back to the positive electrode and so forth. The bouncing speed in the static field increases with the applied electric-field. In our strong electric-field, this speed is too high for the formation of chains or columns. On the other hand, in the ac field, particles mostly oscillate locally; therefore, there is a chance to form chains and columns.

(b) The real part of superconductor's conductivity has a δ function at $\omega=0$ and is vanishing for $0<\omega<\omega_g$ within the superconducting energy gap. Therefore, a chain or column between the two electrodes at $\omega>0$ does not lead to the electrical breakdown, while the infinite real part of the conductivity at $\omega=0$ makes such a chain or column unsustainable.

(3) Once the applied electric-field was further increased to reach a critical value, the chains and columns suddenly broke into pieces, moving between the two electrodes like clouds. However, after several milliseconds, these particles aggregated into macroscopic balls (Fig. 5). The value of this field was marked as E_{c1} same as in the static field. At frequency below 450 Hz, especially $f\leqslant 100$ Hz, the balls bounced between the two electrodes, quite similar to the situation in the static field, although the speed was slower than that in the static field. This bouncing indicated that the balls possessed some net charge on them. At a higher frequency, the balls just oscillated locally and collided with the electrodes occasionally. If f was close to 800 Hz, the oscillation amplitude was very small and collisions with the electrodes were rare, indicating the net charge on the balls was little. In all cases, for $E\geqslant E_{c1}$, layers of HTSC particles were also formed on each electrode almost simultaneously with the ball formation. After turning off the electric-field, both balls and layers became very fragile. If we shook the cell slightly, the balls and layers were all broken.

Figures 6, 7, and 8 show the critical field E_{c1} versus ac frequency for BSCCO, NBCO, and YBCO, respectively. It is clear that the critical field E_{c1} for all these materials had similar behavior as f increased. First, E_{c1} sharply dropped from the value for the static field ($f=0$) to reach a minimum, then rose monotonically as f was further increasing. For example, E_{c1} was 760 V/mm in the static field for NBCO; it dropped to 117 V/mm at 10 Hz, reached 144 V/mm at 15 Hz, climbed to 154.5 V/mm at 25 Hz. Further increasing f led to monotonically increase of E_{c1}. The behavior of E_{c1} for BSCCO and YBCO was quite similar. The minimum of E_{c1} for these materials seemed to be all around or below 10 Hz although the precise position has to be determined yet.

For all three HTSC materials, as shown in Figs 6–8, E_{c1} increased with the frequency almost linearly except the region near the minimum. We also noted that the BSCCO particles seemed to be less affected by the frequency of ac field

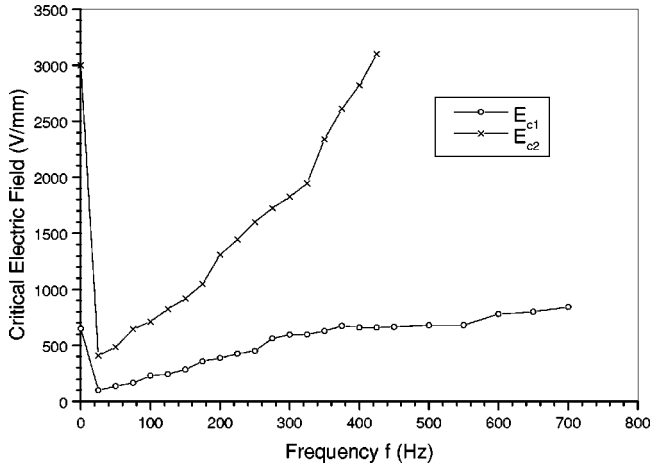

FIG. 6. The critical fields E_{c1} and E_{c2} vs ac frequency f for BSCCO.

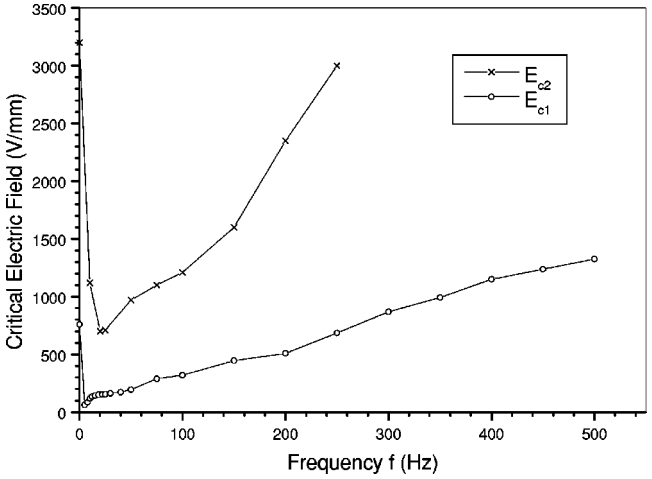

FIG. 7. The critical fields E_{c1} and E_{c2} vs ac frequency f for NBCO.

than the NBCO and YBCO particles. The slope of the E_{c1} curve after $f>25$ Hz in Fig. 6 is smaller than that in Figs. 7 and 8. In fact, E_{c1} at $f=500$ Hz is 0.68 kV/mm for BSCCO and 1.38 kV/mm for NBCO, respectively.

(4) For frequency $f<400$ Hz, further increase of E would lead the bouncing balls to break into small pieces when E rises to the second critical value (Figs. 6and 7). This electric-field was denoted as E_{c2}, same as in the case of static field. At low frequency, especially $f\leqslant 100$ Hz, these small pieces were bouncing between the two electrodes and eventually stuck to the electrodes.

The critical field E_{c2} versus ac frequency was in Fig. 6 for BSCCO and in Fig. 7 for NBCO. It is clear that for both materials, E_{c2} had a sharp drop from the value at the static field $(f=0)$, then increased rapidly with f. However, for BSCCO, E_{c2} was too high to be measured after $f>450$ Hz: in fact, it must have been higher than the dielectric breakdown field so that we could not reach it in the experiment. The situation of E_{c2} for NBCO was similarly too high after $f>250$ Hz. For YBCO, the value of E_{c2} was quite high for the whole range and very difficult to determine since a dielectric breakdown often occurred before E_{c2} was reached. Therefore, we did not plot E_{c2} in Fig. 8 .

The above phenomenon related to E_{c2} was not difficult to be explained by our theory. As discussed in detail later, E_{c2} is related to the dominance of Coulomb interaction, which is required to have some net charge on the ball. In an ac field, the higher the frequency, the smaller the net charge on the balls, and hence the higher the value of E_{c2}.

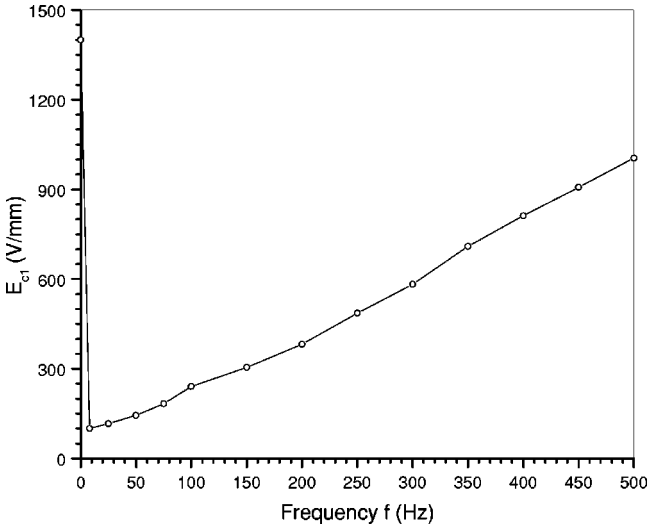

FIG. 8. The critical field E_{c1} vs ac frequency f for YBCO.

C. Particle Surface

The BSCCO, NBCO, and YBCO particle surfaces were easy to deteriorate once they are exposed. An insulating surface layer began to grow during the deterioration. This was from some reaction between carbon atoms in air or environment with the oxygen atoms in the superconducting materials. As reported in Ref. 1, once the particle surface became insulating, the ball formation stopped. This is not difficult to understand. The ball formation requires redistribution of surface charge in order to minimize the surface energy. Once the surface becomes nonconductive, the surface charge cannot be redistributed even if the particles are aggregated together. Then the ball-formation phenomenon disappears.

Our experiment on YBCO particles was especially illustrative. When fresh YBCO particles were placed in liquid nitrogen, they quickly formed macroscopic balls in a strong electric-field. However, if the experimental cell was exposed in air, after about 1 or 2 min, the balls got smaller and smaller during the collision with the electrodes. This indicated that the particle surface was deteriorating due to the exposure to the air. However, if the experiment was performed under nitrogen gas inside a glove box, the YBCO ball was stable, indicating the surface deterioration slowed down

After the HTSC particle surfaces were deteriorated, we conducted the heat treatment on the samples. Oxygen gas was used to reactivate the surface. Once the surface became superconductive, the retreated particles resumed the ball formation in a strong electric field.

D. The ball size and surface energy

In the ac field the balls did not bounce between the two electrodes very fast. This provided an opportunity for us to study the ball shape and ball size. The experiment found that the balls were very round. While the ball size was reducing as the applied electric field was increasing, the spherical shape was unchanged with the field.

As shown in Figs. 9–11, the ball radius R generally decreases with increase of the electric-field. This was consistent with the situation in the static field reported in Ref. 1. In addition, the frequency also plays an important role in the ac case.

For $f<100$ Hz, the relationship between the ball size and the electric-field is almost the same as that in a static field, $E^2R=16\pi\sigma/[(\gamma^2+3)\kappa_L]$, where $\kappa_L=1.44$ is the dielectric constant of liquid nitrogen. Since $\gamma ER^2\kappa_L$ is the net charge on the ball, we take $\gamma\approx 0$ for the ball in the ac field. Then, we would have

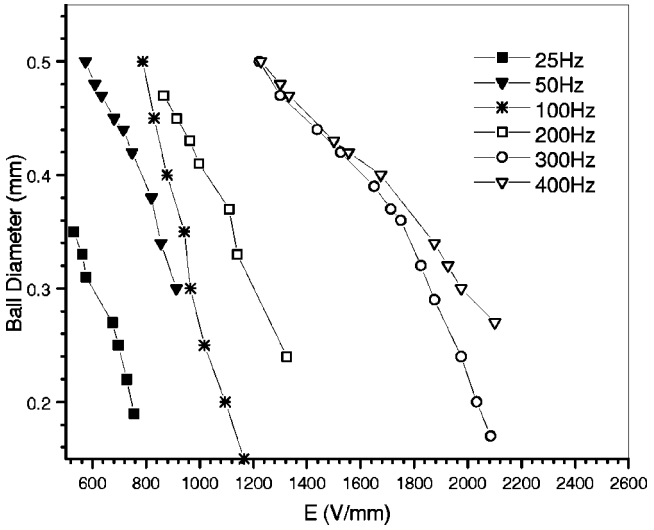

FIG. 9. The BSCCO ball size R vs electric-field E at various frequencies.

$$E^2R=16\pi\sigma/(3\kappa_L). \tag{1}$$

In fact, a careful examination finds that at $f<100$ Hz, $R\sim 1/E^2$ holds quite well. Using Eq. (1), we estimate that the surface energy density is about 14.8×10^{-3} N/m for BSCCO, 11.8×10^{-3} N/m for NBCO, and 6.3×10^{-3} N/m for YBCO at $f=50$ Hz respectively. These values for BSCCO, NBCO, and YBCO at 50 Hz are slightly higher than the values of these materials in a static field.

However, at high frequency the situation was different. If $f\geqslant 100$ Hz, the radius R does not decrease as fast as $1/E^2$. As discussed for the static case, the ball size is determined by the minimization of the positive surface energy, the Coulomb energy, and the polarization energy. In the static field, as noted in Ref. 1, the charge on the ball is well defined. In the ac field, the net charge on the ball is small, but not vanishing and not well defined. If there is more net charge on a ball, the ball size will reduce. Therefore, the ball size in an ac field varies more than that in a static electric-field.

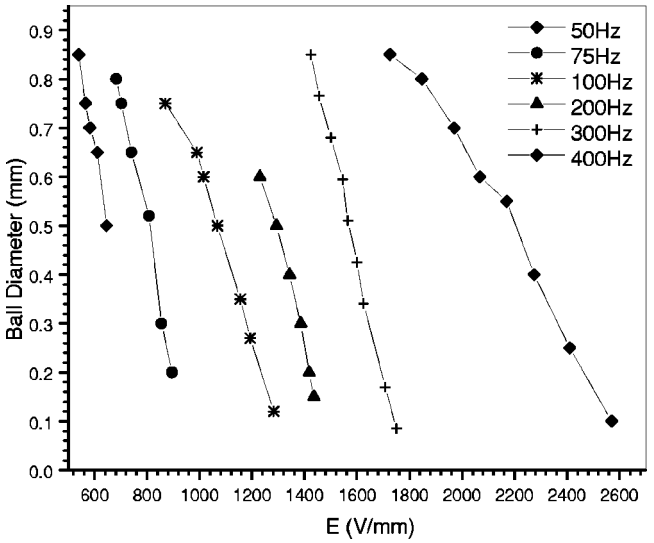

FIG. 10. The NBCO ball size R vs electric-field E at various frequencies.

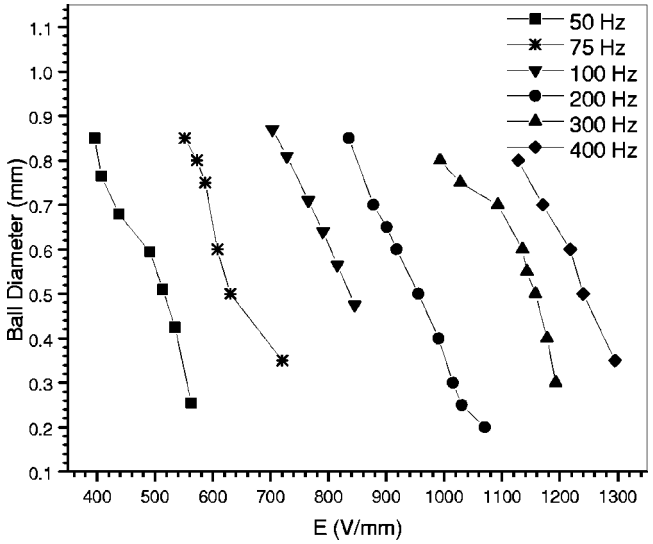

FIG. 11. The YBCO ball size R vs electric-field E at various frequencies.

III. PRELIMINARY THEORETICAL EXPLANATION

Our current theoretical understanding of the phenomenon is far from satisfactory. We will discuss our theoretical understanding related to the static electric-field first. Afterwards, we will extend it to the situation of ac field.

When the superconducting particles are in an electric-field, there are induced charge distributions near the particle surface. Associated with the charge distributions, the electric-field also penetrates inside the superconductors. Let us assume that the screening length of electric-field penetrating into the superconductor is l_s, then the electric-field inside the superconductor can be estimated as

$$\vec{E}(x)=E(x)\vec{e}_x\sim\vec{e}_xE\exp(-x/l_s), \tag{2}$$

where $\vec{e}_x$ is the unit normal of the surface pointing to the inside of the superconductor, x is the depth from the surface into the superconductor, and E is the electric-field just outside the surface.

A Cooper pair is a coupled pair of electrons with opposite spins at average distance of ξ, where ξ is the superconductor's coherent length. The binding energy of the Cooper pair at temperature T is Δ, $\Delta(T)=2\epsilon_f-\epsilon$, where ϵ_f is the Fermi energy and ϵ is the eigenvalue for the pair. Roughly speaking, if the following condition is satisfied

$$e\int_0^{\xi}E(x)dx>\Delta(T), \tag{3}$$

the Cooper pair is depleted because the presence of electric-field makes the energy difference between these two electrons bigger than their binding energy Δ. Assuming $\xi\gg l_s$, we then have E_{c1} given by

$$E_{c1}\sim\Delta(T)/(el_s). \tag{4}$$

The condition $\xi \gg l_s$ implies a sharp boundary between the normal region N and the superconducting region *S*. The normal region has a thickness $\sim\xi$. When considering the change of thermal energy due to the creation of this *N* region, we treat it as that the superconductivity is damaged in a region of thickness $\sim\xi$ at the surface. Thus we lose the condensation energy $\Delta(T)n_s(T)$ over an interval $\sim\xi$, where $n_s(T)$ is the Cooper pair density at temperature *T*. This gives the surface energy per unit area

$$\sigma=\Delta(T)n_s(T)\xi=eE_{c1}n_s(T)l_s\xi. \tag{5}$$

We now consider how to determine the ball size. When a ball bounces between the two electrodes, it picks some net charge *q*. We assume $|q|=\gamma E_0 a_t^2\kappa_L$, where a_t is the ball radius when it hits the electrodes, γ is a constant, and E_0 is the applied electric field. In a static field, γ is related to the deformation of the ball during the collision with the electrodes. For example, if the ball is rigid when colliding with the electrode, it discharges first and then picks up a charge close to $3\kappa_L E_0 a_t^2/4=0.75\kappa_L E_0 a_t^2$ as it leaves the electrode. If the ball is, similar to a droplet, soft enough to deform into a hemisphere with its flat surface in full contact with the electrode, it picks up a charge close to $3(4)^{1/3}\kappa_L E_0 a_t^2/4 = 1.19\kappa_L E_0 a_t^2$ as it leaves the electrode. On the other hand, from the ball's bouncing speed between the two electrodes, we can estimate the actual charge on the ball. The real situation in the static electric-field is found to be between these two extreme cases and $\gamma\approx 1$.

If a ball has radius *R* and net charge *q* in the middle of the capacitor, away from the two electrodes, the total energy is given by

$$U=4\pi\sigma R^2+q^2/(2\kappa_L R)-E_0^2R^3\kappa_L/2. \tag{6}$$

The second term is the Coulomb energy, while the third term is the polarization energy. The net charge on the ball is fixed before the next time it collides with the electrode. A ball made of granular particles has some freedom to fluctuate its size between two consequent collisions in a static field. The radius of a stable ball inside the static electric-field is thus determined by minimization of *U*. From $\partial U/\partial R=0$, we then have

$$\sigma=q^2/(16\pi R^3\kappa_L)+3E_0^2R\kappa_L/(16\pi). \tag{7}$$

Substitute $|q|$ here. While Eq. (6) is not applicable to the situation when the ball collides with the electrodes, a_t and *R* should be almost the same. We then have

$$E_0^2R=16\pi\sigma/[(\gamma^2+3)\kappa_L]. \tag{8}$$

This equation fits the experimental result for static electric-field quite well.

Let us consider E_{c2} for a static electric-field now. If a ball of radius *R* splits into two identical smaller balls, new ball will have radius $R/2^{1/3}$ and charge $q/2$. Then similar to Eq. (6), the total energy of these two balls is given by

$$U'=2^{7/3}\pi R^2\sigma+q^2/(2^{5/3}\kappa_L R)-E^2R^3\kappa_L/2. \tag{9}$$

The Coulomb interaction favors the ball breaking. If $q^2>2^{11/3}\pi R^3\sigma\kappa_L/(1+2^{1/3})$, we have $U'<U$; then, the original ball breaks. Using $|q|=\gamma E_0R^2\kappa_L$, we have

$$E_{c2}\sim\left[\frac{2^{11/3}\pi\sigma}{R_i\gamma^2\kappa_L(2^{1/3}+1)}\right]^{1/2}, \tag{10}$$

where R_i is the minimum size of balls which can be observed in our experiment.

Now let us extend the above discussions to the situation of ac field preliminarily. The electric-field is now time dependent. The expression for electric-field inside the superconductor, Eq. (2), is thus modified:

$$\vec{E}(x)=E(x)\vec{e}_x\cos(\omega t)\sim\vec{e}_xE\exp(-x/l_s)\cos(\omega t). \tag{11}$$

Since $\nabla\times\vec{E}=0$, there is no magnetic field inside the superconductor. Let the Hamiltonian for a pair of electrons with no electric field be $H_0=(p_1^2+p_2^2)/(2m)+V_0$, where V_0 includes the electron-electron interaction and other interactions. To add the interaction between the pairs and the electric-field, we have a time-dependent Hamiltonian

$$H(t)=H_0+e[V(x_1)+V(x_2)]\cos(\omega t), \tag{12}$$

where $V(x)=(E/l_s)\exp(-x/l_s)$. If the electric-field is very weak, from the time-dependent Schrödinger equation

$$i\hbar\,\partial\psi/\partial t=H(t)\psi, \tag{13}$$

under the influence of time-dependent electric-field, the pair's energy is hopping between $\epsilon-\hbar\omega$, ϵ, and $\epsilon+\hbar\omega$, where ϵ is the pair's energy with no ac electric-field. If the ac electric-field is strong, the pair's energy can be $\epsilon\pm\hbar\omega, \epsilon\pm 2\hbar\omega$, $\epsilon\pm 3\hbar\omega$, ... In our case, since the applied electric-field is very strong, the pair's energy is ranged between $\epsilon-\beta\hbar\omega$ to $\epsilon+\beta\hbar\omega$, where β is a constant, $\beta\gg 1$. The strongest binding of the Cooper pair is at the time when the pair has the lowest energy, $\epsilon-\beta\hbar\omega$, which corresponds to a binding energy $2\epsilon_f-(\epsilon-\beta\hbar\omega)=\Delta(T)+\beta\hbar\omega$. In order to deplete all Cooper pairs near the surface, it requires the following condition:

$$e\int_0^{\xi}E(x)dx>2\epsilon_f-(\epsilon-\beta\hbar\omega)=\Delta(T)+\beta\hbar\omega. \tag{14}$$

Hence E_{c1} is estimated as

$$E_{c1}(\omega)\sim[\Delta(T)+\beta\hbar\omega]/(el_s). \tag{15}$$

The above results explain our experiments. First, the electric-field penetration depth to superconductors l_s of an ac field is much longer than that of a static field even if $\omega=2\pi f$ is not very high. There is already some experimental evidence to support the claim.[13,9] This accounts for the short drop of E_{c1} from $\omega=0$ to $\omega>0$ in Figs. 6–8. Currently it is unknown if or how l_s changes with ω. Since the frequency in our experiments only varies from $0+$ to several hundred hertzs, we can safely assume that l_s varies little during this range. Then, E_{c1} increases with the frequency of the applied field approximately linearly with a slope $\beta\hbar/(el_s)$. An examination of

Figs. 6–8 seems to confirm the above expression. The constant $\beta\hbar/(el_s)$ is about 0.175 for BSCCO, 0.399 for NBCO, and 0.298 for YBCO. The constant β is estimated about 10.[10] We note that although $\beta \gg 1$, $\beta\hbar\omega$ is still much smaller than $\Delta(T)$, the binding energy.

In an ac field, the net charge on a ball $|q| = \gamma E_0 R^2 \kappa_L$ is small. Thus, the constant γ is small. Basically, a ball inside the capacitor will remain neutral if there are no collisions between the ball and electrodes. In the ac field, the electric-field changes its polarity after π/ω, half period. The chance of collisions between a ball and the electrodes depends on the distance that the ball is able to move during such an interval π/ω. If the electric-field strength remains the same for all frequencies, the chance of such collisions decreases as the frequency ω gets higher. Therefore, γ is a function of frequency ω. From the above arguments, we can roughly estimate that γ decreases at least as fast as $1/\omega$. If we take this estimation into Eq. (10), we understand why E_{c2} is very high in ac field and increases with ω. This is consistent with the E_{c2} results in Figs. 6 and 7.

The estimation of l_s for superconductors is a difficult issue. However, from our experimental results of $E_{c1}$and σ, we can apply Eq. (5) to make a rough estimation. At $f = 50$ Hz, l_s is about several hundred angstroms for all three HTSC materials used in our experiment.

IV. SUMMARY

In concluding the present paper, we would point out that the frequency in our experiment is quite low, but its effect on the critical field and ball size is significant. The phenomenon has many similarities to that in the static electric-field, but also possesses some distinct features. For all our HTSC powders, the critical field E_{c1} first drops from the value for a static electric-field, then increases with the frequency. The ball size reduces if the field strength further increases. When the frequency is low, such as below 100 Hz, the relationship between the ball size and the electric-field is almost the same as that in the static field. However, when the frequency is high, the ball size in the ac field decreases with the field more slowly than that in the static field. For quite low frequencies, similar to the static electric-field, there is another critical field E_{c2} with $E_{c2} > E_{c1}$. If the applied electric-field exceeds E_{c2}, all the balls break into pieces. E_{c2} increases rapidly with the frequency and soon exceeds the field to cause dielectric breakdown.

In our experiments, we further confirm that the HTSC particle surface must be conductive for the ball formation. This is required to redistribute the surface charge in minimizing the surface energy. The heat treatment can eliminate the deteriorated surface layer and make the HTSC particles reactive in the ball formation.

The experimental results in the ac field present some challenges to the theory. Our current theoretical understanding is preliminary, providing some explanations for the experimental results. Detailed calculations are needed for further quantitative comparison between the theory and experiment. Some of our experimental results, for example, the relationship between E_{c1} and the frequency and the relationship between the ball size and the frequency, demand further development of a microscopic theory.

ACKNOWLEDGMENTS

We wish to thank Dr. Y. Lan, E. Kaczanowicz, S. Murray, and Y. Shiroyanagi for their assistance. This research was supported by NSF Grant No. DMR-0075780.

[1] R. Tao, X. Zhang, X. Tang, and P.W. Anderson, Phys. Rev. Lett. **83**, 5575 (1999).
[2] I. Peterson, Sci. News (Washington, D.C.) **157**, 21 (2000).
[3] J.E. Hirsch, Phys. Lett. A **281**, 44 (2001).
[4] T.J. Yang and W.D. Lee, Physica C **364**, 166 (2001).
[5] R. Tao, X. Xu, Y.C. Lan, and Y. Shiroyanagi, Physica C **3776**, 357 (2002).
[6] F. Landau and H. London, Proc. R. Soc. London, Ser. A **152**, 24 (1935); H. London, *ibid.* **155**, 102 (1936).
[7] I.L. Landau, Sov. Phys. JETP **11**, 295 (1970).
[8] A.B. Pippard, J.G. Shepherd, and D.A. Tindall, Proc. R. Soc. London, Ser. A **324**, 17 (1971).
[9] S.N. Artemenko and A.F. Volkov, Sov. Phys. Usp. **22**, 295 (1979).
[10] J.G. Bednorz and K.A. Müller, Z. Phys. B: Condens. Matter **64**, 189 (1986).
[11] M.K. Wu, J.R. Ashburn, C.J. Torng, P.H. Hor, R.L. Meng, L. Gao, Z.L. Huang, Y.Q. Wang, and C.W. Chu, Phys. Rev. Lett. **58**, 908 (1987).
[12] For example, see, T. Frey, J. Mannhart, J.G. Bednorz, and E.J. Williams, Phys. Rev. B **51**, 3257 (1995); S. Sakai, *ibid.* **47**, 9042 (1993); T.J. Yang and W.D. Lee, Physica C **341-348**, 291 (2000).
[13] W.G. Jenks and L.R. Testardi, Phys. Rev. B **48**, 12 993 (1993).
[14] U. Balachandran, R.B. Poeppel, J.E. Emerson, S.A. Johnson, M.T. Lanagan, C.A. Youngdahl, D.L. Shi, K.C. Goretta, and N.G. Eror, Mater. Lett. **8**, 454 (1989).
[15] B.C. Bunker, J.A. Voigt, D.H. Doughty, D.L. Lamppa, and K.K. Kimball, in *High Temperature Superconducting Materials: Preparation, Properties and Process*, edited by W.E. Hatfield and J.H. Miller, Jr. (Marcel Dekker, New York, NY, 1988), p. 121.
[16] T.J. Chen, X. Zhang, and R. Tao, Int. J. Mod. Phys. B **13-14**, 1697 (1999).